

Supporting Information

Rare-earth-metallocene alkylaluminates trigger distinct tetrahydrofuran activation

Martin Bonath, Verena M. Birkelbach, Christoph Stuhl, Cäcilia Maichle-Mössmer,
and Reiner Anwander*

*Institut für Anorganische Chemie, Universität Tübingen, Auf der Morgenstelle 18, D-72076 Tübingen,
(Germany)*

* E-mail for R. A.: reiner.anwander@uni-tuebingen.de

Table of Contents

Experimental Section	S3
General Considerations	S3
Synthesis of 1	S3
Synthesis of 2	S4
Synthesis of 3	S4
Synthesis of 4	S4
Synthesis of 5	S5
Figure S1. Crystal structure and structural parameters of 2	S6
Figure S2. Crystal structure and structural parameters of 3	S6
Figure S3. Crystal structure and structural parameters of 4	S7
Figure S4. Crystal structure and structural parameters of 5	S7
Table S1. Crystallographic data for 2 , 3 , 4 and 5	S8
Figure S5. ^1H NMR spectrum of 2	S9
Figure S6. $^{13}\text{C}\{^1\text{H}\}$ NMR spectrum of 2	S9
Figure S7. ^1H NMR spectrum of 3	S10
Figure S8. $^{13}\text{C}\{^1\text{H}\}$ NMR spectrum of 3	S10
Figure S9. ^1H - ^1H COSY NMR spectrum of 3	S11
Figure S10. ^1H - ^{13}C HSQC NMR spectrum of 3	S11
Figure S11. ^1H NMR spectrum of crude product mixture of 2 and 3 in C_6D_6	S12
Figure S12. ^1H NMR spectrum of crude product mixture of 2 and 3 in $\text{THF-}d_8$	S12
Figure S13. ^1H NMR spectrum of 1 in C_6D_6 after heating to $90\text{ }^\circ\text{C}$ for 11 h	S13
Figure S14. ^1H NMR spectrum of 1 in C_6D_6 after heating to $90\text{ }^\circ\text{C}$ for 11 h and evaporation	S13
Figure S15. ^1H NMR spectrum of 4	S14
Figure S16. $^{13}\text{C}\{^1\text{H}\}$ NMR spectrum of 4	S14
Figure S17. ^1H NMR spectrum of 5	S15
Figure S18. $^{13}\text{C}\{^1\text{H}\}$ NMR spectrum of 5	S15
Figure S19. ^1H - ^1H COSY NMR spectrum of 5	S16
Figure S20. ^1H - ^{13}C HSQC NMR spectrum of 5	S16
Figure S21. ^1H NMR spectrum 4 in C_6D_6 , after addition of $\text{THF-}d_8$	S17
References	S18

Experimental Section

General Consideration. Syntheses and manipulations of all organometallic compounds were carried out under dry argon by using standard *Schlenk*, high-vacuum, and glovebox techniques (MBraun MB 200B; <1 ppm O₂, <1 ppm H₂O). *n*-Pentane, *n*-hexane, toluene and tetrahydrofurane (THF) were purified by using *Grubbs* columns (MBraun SPS-800, solvent purification system) and stored in a glovebox. C₆D₆ and THF-*d*₈ were obtained from Aldrich, dried over Na/K alloy for 24 h and distilled prior to use. AlMe₃ was purchased from Aldrich, Me₃SiI was purchased from abcr and used as received. Cp*₂Y(AlMe₄) and Cp*₂La(AlMe₄) were synthesized according to literature procedures.¹ NMR spectra of air and moisture sensitive compounds were recorded by using J. Young valve NMR tubes at 26 °C on a *Bruker* AVII+250 (¹H: 250.13 MHz; ¹³C: 62.90 MHz), and on a *Bruker* AVII+400 (¹H: 400.13 MHz; ¹³C: 100.61 MHz). ¹H and ¹³C NMR shifts are referenced to internal solvent resonances and reported in parts per million (ppm) relative to TMS. IR spectra were recorded on a NICOLET 6700 FTIR spectrometer using a DRIFT chamber with dry KBr/sample mixtures and KBr windows. For the latter the collected data were converted using the Kubelka-Munk refinement. Elemental analyses were performed on an *Elementar Vario MICRO cube*. Suitable crystals for X-ray structure analyses were selected in a glovebox and coated with Parabar 10312 (previously known as Paratone N, Hampton Research) and fixed on a nylon loop/glass fiber. X-ray data were collected on a Bruker APEX II DUO diffractometer by using QUAZAR optics and MoK_α radiation ($\lambda = 0.71073 \text{ \AA}$). The data collection strategy was determined using COSMO² employing ω -scans. Raw data were processed by using APEX³ and SAINT⁴ software; structure solution and final model refinement were performed by using SHELXL⁵ and ShelXle.⁶ Corrections for absorption effects were applied by using SADABS.⁷ All nonhydrogen atoms were refined anisotropically. Disorder models were calculated using DSR,⁸ a program for refining disordered structures in ShelXl. All plots were generated utilizing the programs ORTEP-3⁹ and POV-Ray.¹⁰ Further details of the refinement and crystallographic data are listed in Table S1, and in the CIF files. CCDC depositions 2087233-2087236 contain all the supplementary crystallographic data for this paper. These data can be obtained free of charge from The Cambridge Crystallographic Data Centre via www.ccdc.cam.ac.uk/structures/.

Cp*₂YMe(thf) (1). The synthesis of **1** was performed in a slightly modified procedure as described in the literature.¹ In a scintillation vial, Cp*₂Y(AlMe₄) (159 mg, 0.36 mmol) was diluted in THF (0.8 mL). Then *n*-hexane (10 mL) was added, the reaction mixture filtered and the filtrate stored at -40 °C. After three days **1** crystallized as colorless crystals. To prevent partial back reaction the cold supernatant was removed, the solids washed with *n*-hexane and dried under reduced pressure to achieve pure **1** (124 mg, 78%). The ¹H NMR spectroscopic data are in accord with literature.¹¹

Cp*₂YMe(OC₂H₃)(thf) (2). In a pressure tube, **1** (118 mg, 0.27 mmol) was dissolved in THF and stirred at 90 °C for three days. Then, all volatiles were removed under reduced pressure to obtain a pale yellow powder as the crude product. According to ¹H NMR spectral data the crude product contained **2** and **3** in an approximate ratio of 3:2. To obtain a pure sample of **2**, the crude product was subjected to fractional crystallization from *n*-pentane. Single crystals suitable for X-ray crystallography were grown from a saturated *n*-pentane solution at -40 °C (71 mg, 57%). ¹H NMR (C₆D₆, 400 MHz, 26 °C): δ = 7.25 (dd, 1 H, ³J(H,H)_{cis} = 5.5 Hz, ³J(H,H)_{trans} = 13.7 Hz, OCH=CH₂), 4.19 (dd, 1 H, ²J(H,H)_{geminal} = 0.6 Hz, ³J(H,H)_{trans} = 13.7 Hz, OCH=CH₂), 4.03 (dd, 1 H, ²J(H,H)_{geminal} = 0.5 Hz, ³J(H,H)_{cis} = 5.7 Hz, OCH=CH₂), 3.49 (m, 4 H, O(CH₂CH₂)₂), 2.01 (s, 30 H, C₅(CH₃)₅), 1.20 (m, 4 H, O(CH₂CH₂)₂) ppm. ¹³C{¹H} NMR (C₆D₆, 101 MHz, 26 °C): δ = 156.0 (OCH=CH₂), 116.8 (d, ¹J(Y,C) = 1.4 Hz, C₅(CH₃)₅), 85.3 (OCH=CH₂), 71.7 (O(CH₂CH₂)₂), 25.4 (O(CH₂CH₂)₂), 11.3 (C₅(CH₃)₅) ppm. DRIFT (KBr): $\tilde{\nu}$ = 3096 (w), 2962 (m), 2901 (s), 2855 (m), 2722 (w), 1614 (vs), 1445 (m), 1486 (m), 1437 (m), 1391 (m), 1377 (m), 1317 (s), 1223 (vs), 1015 (m), 999 (s), 862 (m), 772 (w) cm⁻¹. Elemental analysis (%) calcd. for C₂₆H₄₁O₂Y (474.52 g mol⁻¹): C 65.81, H 8.71. Found: C 66.00, H 8.72.

Cp*₂YMe(2-C₂H₄-OC₄H₇) (3). The residual supernatants from the crystallization of compound **2** were condensed, washed with toluene and recrystallized from *n*-pentane to afford pure samples of **3**. Single crystals suitable for X-ray crystallography were grown from a saturated *n*-pentane solution at -40 °C (44 mg, 36%). ¹H NMR (C₆D₆, 400 MHz, 26 °C): δ = 3.73 (m, 1 H, OCH(CH₂)₂), 3.15 (m, 1 H, OCH₂CH₂), 3.07 (m, 1 H, OCH₂CH₂), 2.50 (m, 1 H, YCH₂CH₂), 2.02 (s, 15 H, C₅(CH₃)₅), 2.00 (s, 15 H, C₅(CH₃)₅), 1.72 (m, 1 H, YCH₂CH₂), 1.41 (m, 1 H, OCH₂CH₂CH₂), 1.34 (m, 1 H, OCH₂CH₂CH₂), 1.24 (m, 1 H, OCH₂CH₂CH₂), 1.03 (m, 1 H, OCH₂CH₂CH₂), 0.45 (m, 1 H, YCH₂CH₂), -0.12 (m, 1 H, YCH₂CH₂) ppm. ¹³C{¹H} NMR (C₆D₆, 101 MHz, 26 °C): δ = 115.9 (C₅(CH₃)₅), 90.6 (OCH(CH₂)₂), 67.8 (OCH₂CH₂), 36.3 (YCH₂CH₂), 31.2 (OCH₂CH₂CH₂), 29.7 (d, ¹J(Y,C) = 51.1 Hz, YCH₂CH₂), 26.5 (OCH₂CH₂CH₂), 11.6 (C₅(CH₃)₅), 11.3 (C₅(CH₃)₅) ppm. DRIFT (KBr): $\tilde{\nu}$ = 2962 (s), 2906 (vs), 2860 (vs), 2791 (m), 2722 (w), 1614 (vs), 1454 (w), 1436 (m), 1377 (w), 1130 (w), 1020 (m), 988 (m), 947 (w), 913 (m), 845 (w), 780 (w), 519 (w) cm⁻¹. Elemental analysis (%) calcd. for C₂₆H₄₁OY (458.52 g mol⁻¹): C 68.11, H 9.01. Found: C 67.28, H 8.90.

NMR-scale reaction of Cp*₂YMe(thf) (1) in C₆D₆. In a J.-Young-valved NMR tube, **1** (20 mg, 0.05 mmol) was dissolved in C₆D₆ (0.5 mL) and kept at 90 °C. After 11 h the colourless solution **had** turned to deep orange and all starting material had been consumed. Under these conditions formation of **2** was not observed. Hence, **3**, (Cp*₂Y)₂(μ-O)¹² and Cp*₂YPh-d₅(thf)/Cp*₂YPh(thf) were identified as the main products in an approximate ratio of 2:1:2. The oxy-bridged dimetallic complex is the least soluble and as such separable. Compounds Cp*₂YPh-d₅(thf)/Cp*₂YPh(thf) are likely formed via C-H-bond activation of C₆D₆/C₆H₆ by complex **3**. See, Figures S13 and S14.

[Cp*₂La{(μ-Me)₂AlMe₂}(thf)]_n (4). In a scintillation vial, Cp*₂La(AlMe₄) (309 mg, 0.62 mmol) was diluted quickly in THF (1.7 mL) at ambient temperature. Then *n*-hexane (10 mL) was added instantly, the mixture filtered and the filtrate stored at -40 °C immediately. After three days colourless crystals of **4** (302 mg, 86%) had grown, suitable for X-ray crystallography. ¹H NMR (C₆D₆, 400 MHz, 26 °C): δ = 4.48 (m, 4 H, O(CH₂CH₂)₂), 1.89 (s, 30 H, C₅(CH₃)₅), 1.31 (m, 4 H, O(CH₂CH₂)₂), -0.28(bs, 12 H, Al(CH₃)₄) ppm. ¹³C{¹H} NMR (C₆D₆, 101 MHz, 26 °C): δ = 68.3 (THF, OCH₂CH₂), 25.6 (THF, OCH₂CH₂), 11.1 (C₅(CH₃)₅) ppm; signals for C₅(CH₃)₅ and Al(CH₃) moieties were not detected. DRIFT (KBr): $\tilde{\nu}$ = 2963 (m), 2903 (vs), 2869 (s), 2803 (w), 2728 (w), 1487 (w), 1436 (m), 1377 (w), 1172 (m), 1023 (s), 992 (s), 920 (w), 870 (w), 720 (s), 671 (w), 595 (w), 565 (w), 544 (m) cm⁻¹. Elemental analysis (%) calcd. for C₂₈H₅₀AlLaO (568.59 g mol⁻¹): C 59.15, H 8.86. Found: C 58.87, H 8.46.

Cp*₂La(2-AlMe₃-OC₄H₇) (5). In a scintillation vial, Cp*₂La(AlMe₄) (117 mg, 0.23 mmol) was suspended in *n*-hexane (4 mL) and THF (1.5 mL). Within 30 minutes the suspension gradually dissolved to form a clear, colourless solution. Then, all volatiles were removed under reduced pressure and **5** (130 mg, 97%) was obtained analytically pure as white powder. Crystals of **5** suitable for X-ray crystallography were obtained from an *n*-hexane solution at -40 °C. ¹H NMR (C₆D₆, 400 MHz, 26 °C): δ = 3.43 (m, 1 H, OCH₂CH₂), 3.35 (m, 1 H, OCH₂CH₂), 2.82 (dd, ³J(H,H)_{gauche} = 4.8 Hz, ³J(H,H)_{anti} = 13.6 Hz, 1H, OCH(AlMe₃)CH₂), 2.15 (m, 1H, OCH(AlMe₃)CH₂), 1.90 (s, 15 H, C₅(CH₃)₅), 1.90 (s, 15 H, C₅(CH₃)₅), 1.79 (m, 1H, OCH(AlMe₃)CH₂), 1.63 (m, 1H, OCH₂CH₂), 1.43 (m, 1H, OCH₂CH₂), -0.06 (bs, 3 H, La(μ-CH₃)Al), -0.36 (bs, 6 H, Al(CH₃)₂) ppm. ¹³C{¹H} NMR (C₆D₆, 101 MHz, 26 °C): δ = 121.1 (C₅(CH₃)₅), 120.9 (C₅(CH₃)₅), 78.3 (OCH(AlMe₃)CH₂), 69.2 (OCH₂CH₂), 30.7 (OCH(AlMe₃)CH₂), 29.6 (OCH₂CH₂), 11.1 (C₅(CH₃)₅), 11.1 (C₅(CH₃)₅) ppm; signals for Al(CH₃) moieties were not detected; probably due to fast exchange processes. DRIFT (KBr): $\tilde{\nu}$ = 2963 (m), 2906 (vs), 2857 (s), 2726 (w), 1436 (m), 1378 (w), 1180 (m), 1063 (w), 1022 (w), 990 (w), 971 (w), 889 (w), 798 (w), 716 (m), 684 (s), 601 (w), 567 (w), 544 (w) cm⁻¹. Elemental analysis (%) calcd. for C₂₇H₄₆AlLaO (552.55 g mol⁻¹): C 58.69, H 8.39. Found: C 58.62, H 8.43.

Crystallographic Details

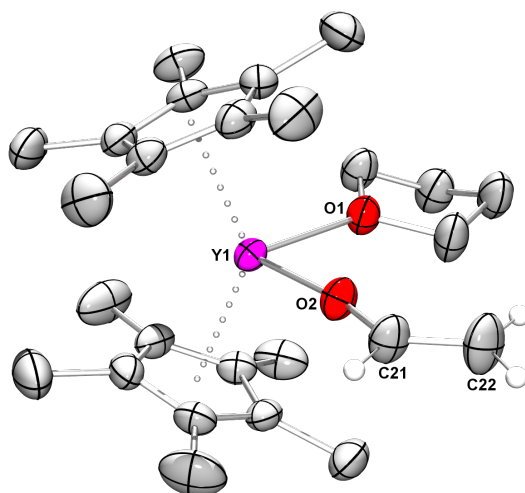


Figure S1. Crystal structure of Cp*₂Y(OC₂H₃)(thf) (**2**). All atoms are represented by atomic displacement ellipsoids set at 50% probability. Hydrogen atoms except at the vinyl alkoxide and disorders in the vinyl alkoxide and the THF molecule are omitted for clarity. Selected interatomic distances [Å] and angles [°]: Y1–O1 2.384(2), Y1–O2 2.08(2), C21–C22 1.33(1); O1–Y1–O2 92.4(4), Y1–O2–C21 171(1).

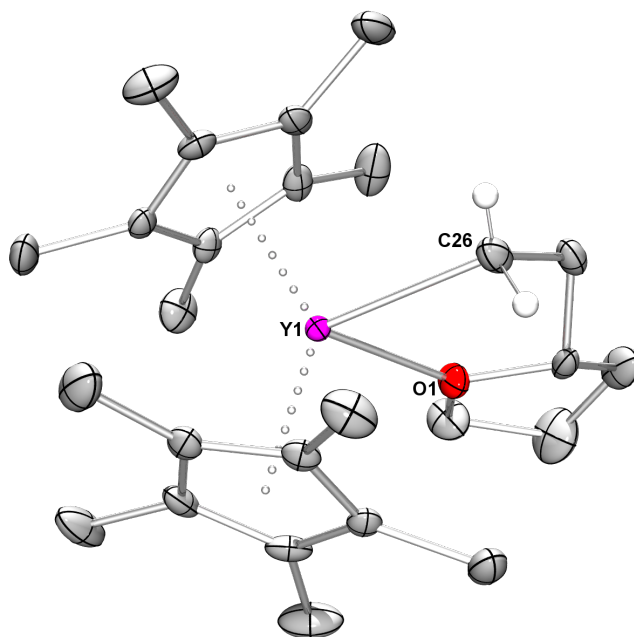


Figure S2. Crystal structure of Cp*₂Y(2-C₂H₄-OC₄H₇) (**3**). All atoms are represented by atomic displacement ellipsoids set at 50% probability. Hydrogen atoms except at C26 and the disorder in the chiral ethylene-2-tetrahydrofuranyl ligand are omitted for clarity. Selected interatomic distances [Å] and angles [°]: Y1–C26 2.439(2), Y1–O1 2.349(1); C26–Y1–O1 73.80(6).

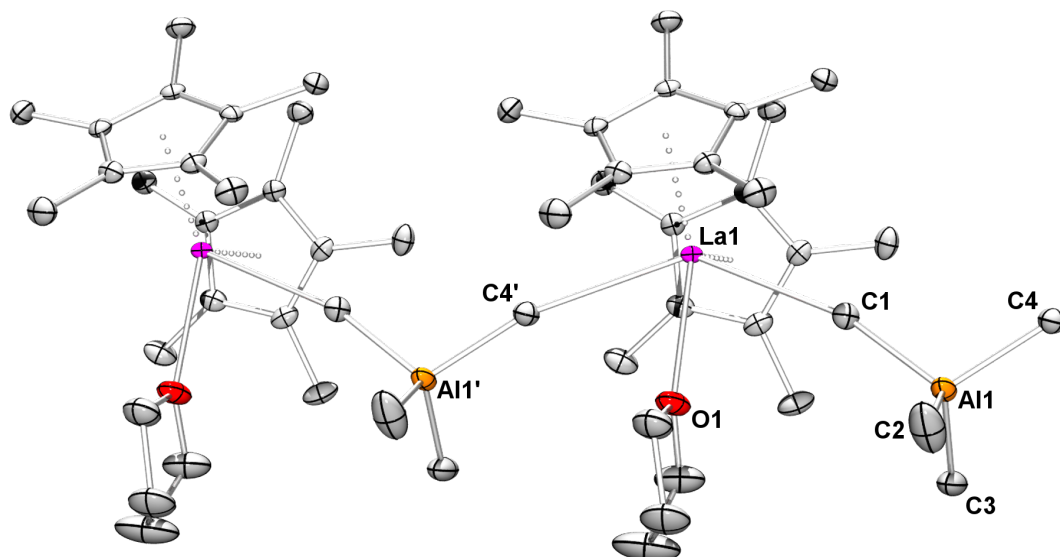


Figure S3. Crystal structure of $[\text{Cp}^*_2\text{La}(\text{AlMe}_4)(\text{thf})]_n$ (**4**). All atoms are represented by atomic displacement ellipsoids set at 50% probability. Hydrogen atoms are omitted for clarity. Selected interatomic distances [\AA] and angles [$^\circ$]: La1–C1 2.910(3), La1–C4' 2.917(3), La1–O1 2.657(2), Al1–C1 2.025(3), Al1–C2 1.974(3), Al1–C3 1.983(3), Al1–C4 2.016(3); Al1–C1–La1 165.4(1), Al1–C4'–La1 166.1(1), C1–La1–C4' 135.64(4).

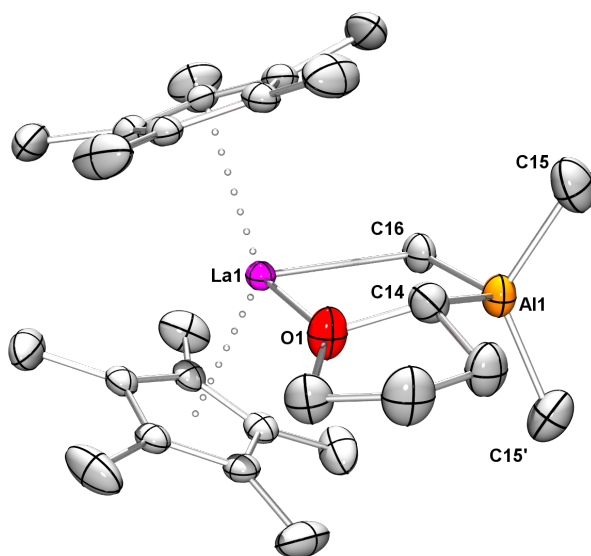


Figure S4. Crystal structure of $\text{Cp}^*_2\text{La}(2\text{-AlMe}_3\text{-OC}_4\text{H}_7)$ (**5**). All atoms are represented by atomic displacement ellipsoids set at 50% probability. Hydrogen atoms and disorder due to co-crystallized enantiomers are omitted for clarity. Selected interatomic distances [\AA] and angles [$^\circ$]: La1–C16 2.753(3), La1–O1 2.425(2), Al1–C14 2.080(4), Al1–C15 1.969(10), Al1–C16 2.048(3), C16–La1–O1 98.14(8), Al1–C16–La1 90.2(1), C14–Al1–C16 114.6(2).

Table S1. Crystallographic data of complexes **2**, **3**, **4** and **5**

	2	3	4	5
Formula	C ₂₆ H ₄₁ O ₂ Y	C ₂₆ H ₄₁ OY	C ₂₈ H ₅₀ AlLaO	C ₂₇ H ₄₆ AlLaO
CCDC	2087233	2087235	2087236	2087234
M _r [g mol ⁻¹]	474.50	458.50	568.57	552.53
cryst syst	orthorhombic	monoclinic	monoclinic	orthorhombic
space group	<i>Pbca</i>	<i>P2₁/n</i>	<i>P2₁/c</i>	<i>Pnma</i>
<i>a</i> [Å]	14.0255(7)	10.5384(2)	18.808(16)	16.6514(15)
<i>b</i> [Å]	16.7687(9)	19.7009(4)	8.677(7)	15.0366(13)
<i>c</i> [Å]	21.8639(15)	11.5448(2)	19.029(16)	11.0355(10)
α [°]	90	90	90	90
β [°]	90	97.1483(10)	113.609(11)	90
γ [°]	90	90	90	90
<i>V</i> [Å ³]	5142.2(5)	2378.25(8)	2845(4)	2763.1(4)
<i>Z</i>	8	4	4	4
<i>T</i> [K]	180(2)	100(2)	100(2)	136(2)
ρ_{calcd} [g cm ⁻³]	1.226	1.281	1.327	1.328
μ [mm ⁻¹]	2.285	2.465	1.548	1.593
F (000)	2016	976	1184	1144
R1/wR2 (I>2 σ) ^[a]	0.0341/0.0714	0.0291/0.0651	0.0274/0.0521	0.0250/0.0576
R1/wR2 (all data) ^[a]	0.0627/0.0809	0.0330/0.0662	0.0420/0.0553	0.0289/0.0596
GOF ^[a]	1.006	1.123	0.935	1.055

[a] R1 = $\Sigma(|F_0| - |F_c|) / \Sigma|F_0|$, $F_0 > 4\sigma(F_0)$. wR2 = $\{\Sigma[w(F_0^2 - F_c^2)^2] / \Sigma[w(F_0^2)^2]\}^{1/2}$.

NMR Spectra

In general solvent peaks are marked with (°) or an asterisk (*).

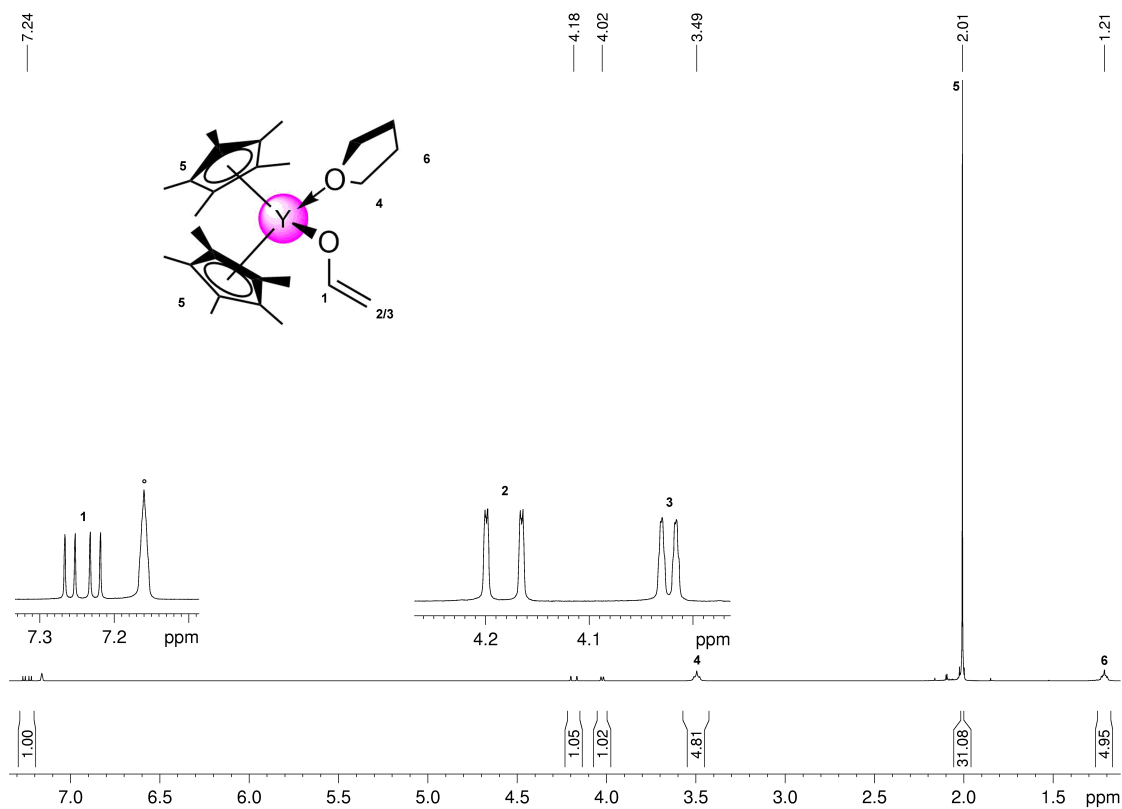


Figure S5. ¹H NMR spectrum (400 MHz) of **2** in C₆D₆ (°) at 26 °C.

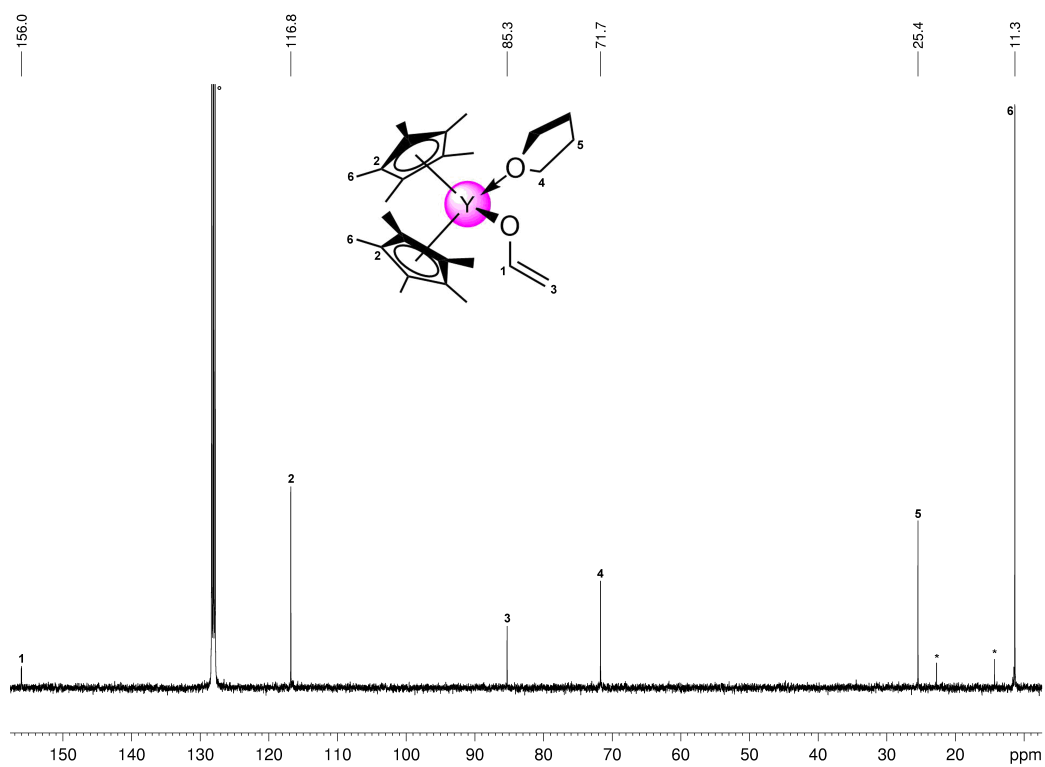


Figure S6. ¹³C {¹H} NMR spectrum (101 MHz) of **2** in C₆D₆ (°) at 26 °C (* *n*-hexane).

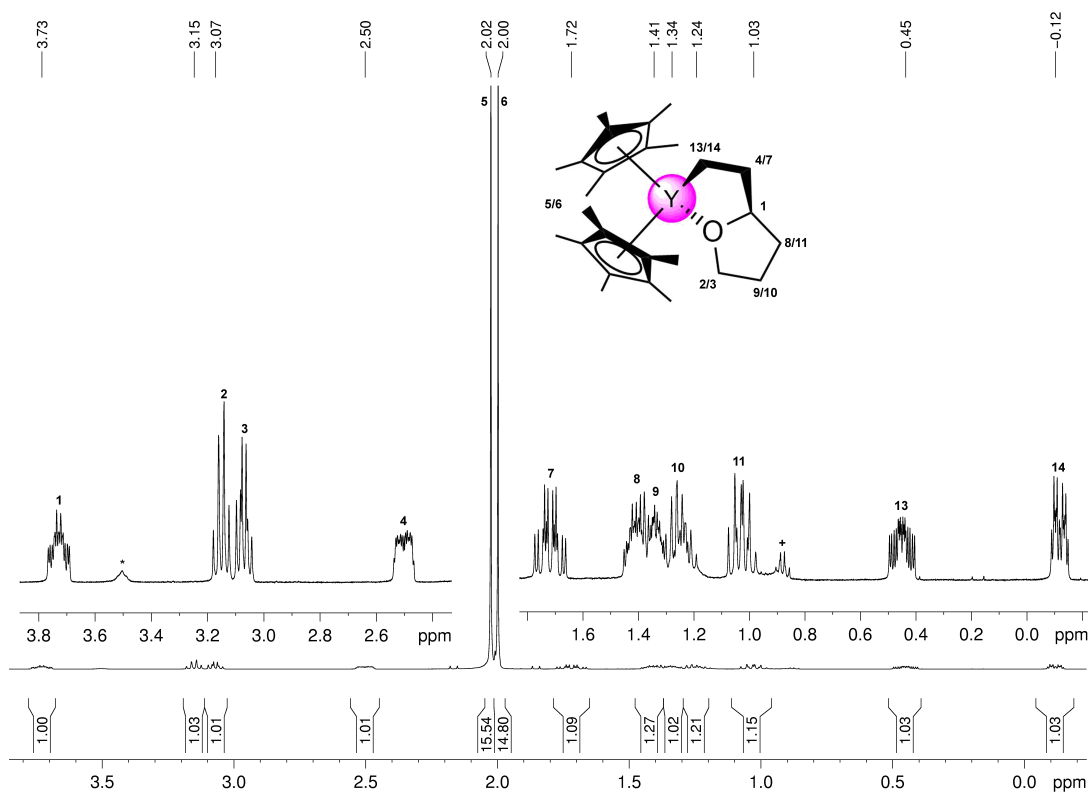


Figure S7. ^1H NMR spectrum (400 MHz) of **3** in C_6D_6 at 26 °C (* THF, + *n*-hexane).

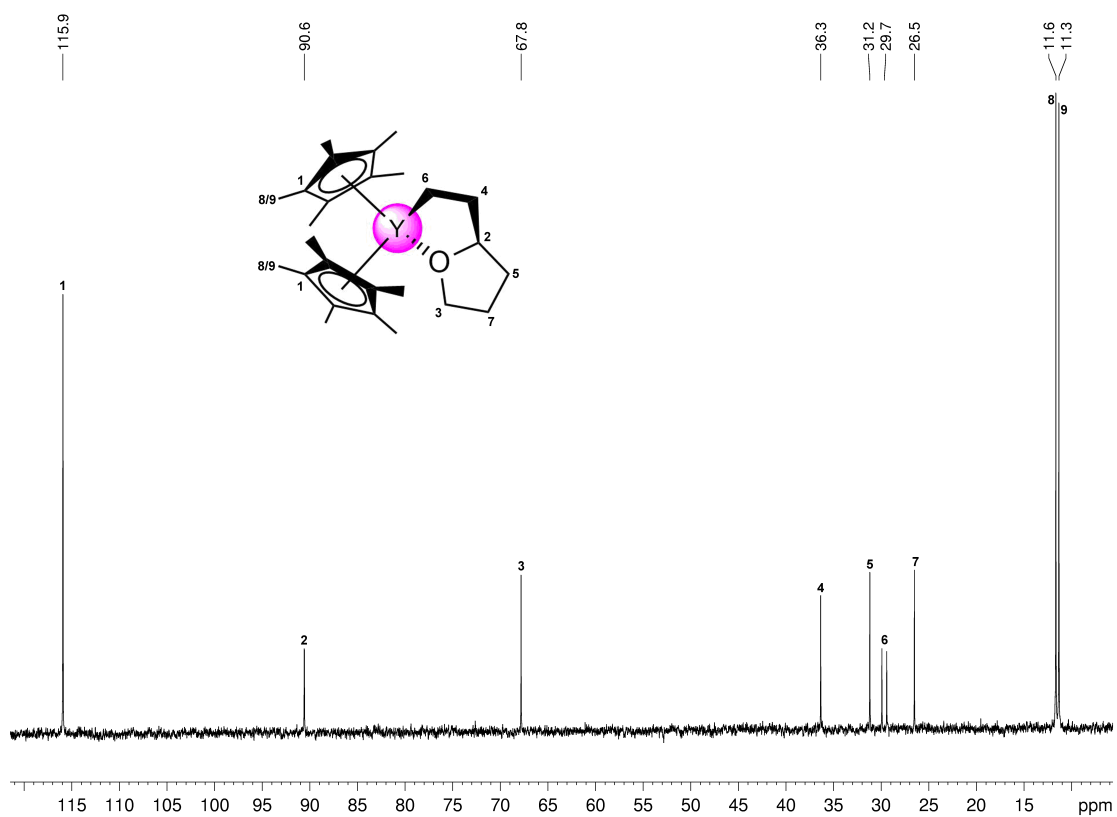


Figure S8. $^{13}\text{C}\{^1\text{H}\}$ NMR spectrum (101 MHz) of **3** in C_6D_6 at 26 °C.

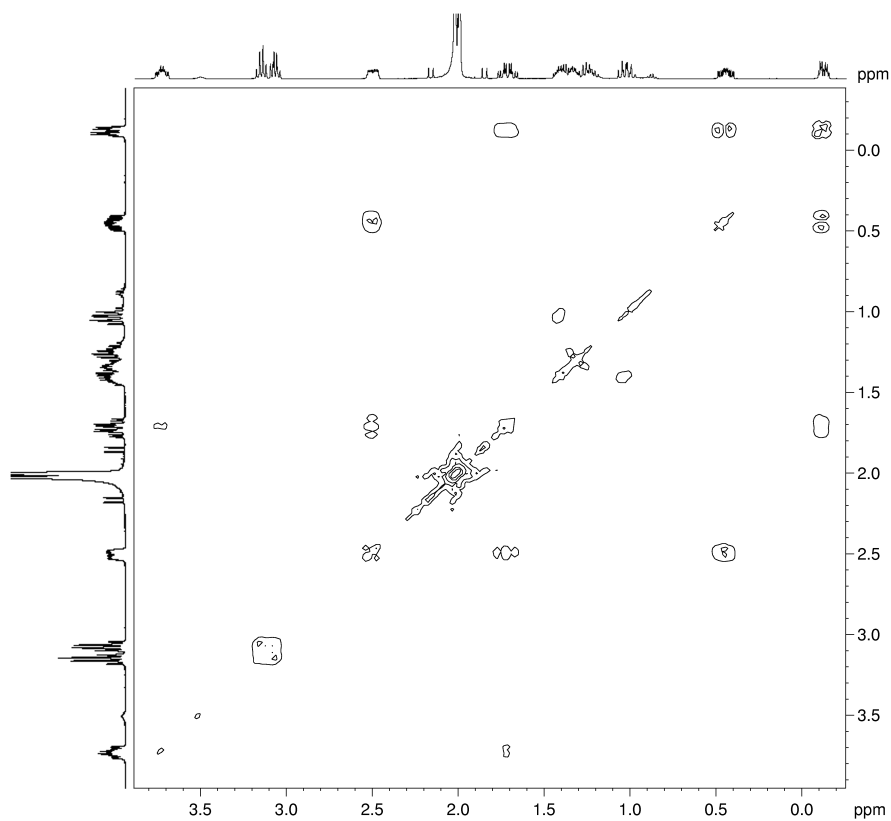


Figure S9. ^1H - ^1H COSY NMR spectrum (400 MHz) of **3** in C_6D_6 at 26 °C.

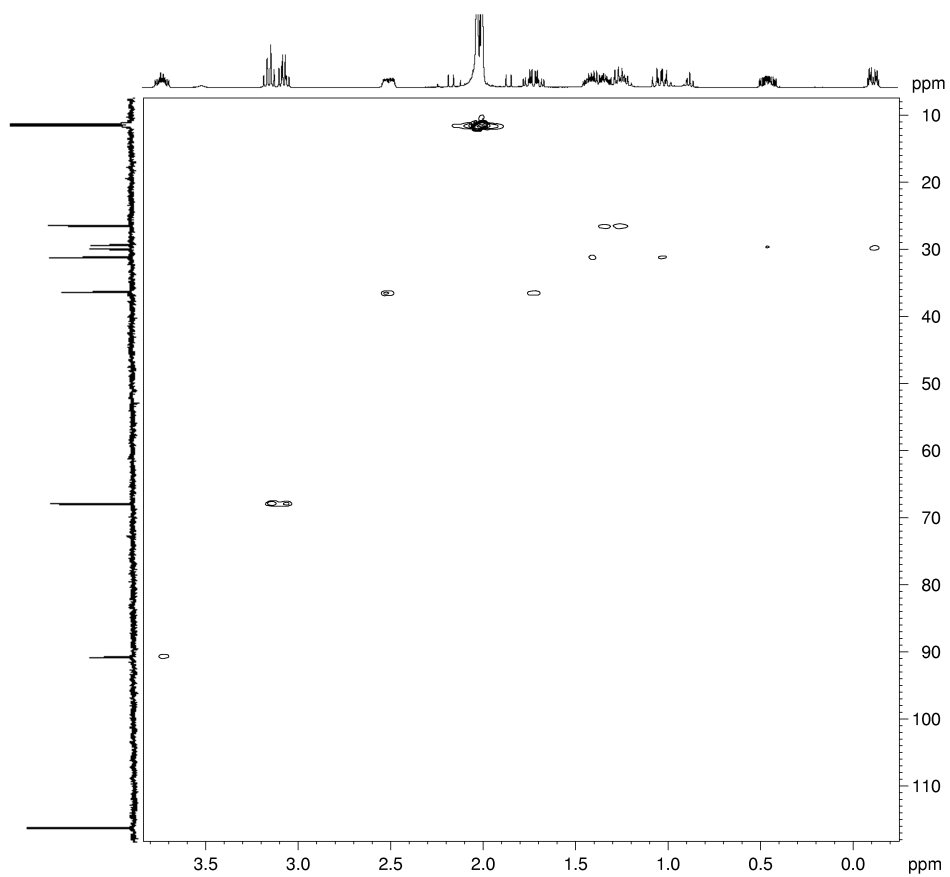


Figure S10. ^1H - ^{13}C HSQC NMR spectrum (400 MHz, 101 MHz) of **3** in C_6D_6 at 26 °C.

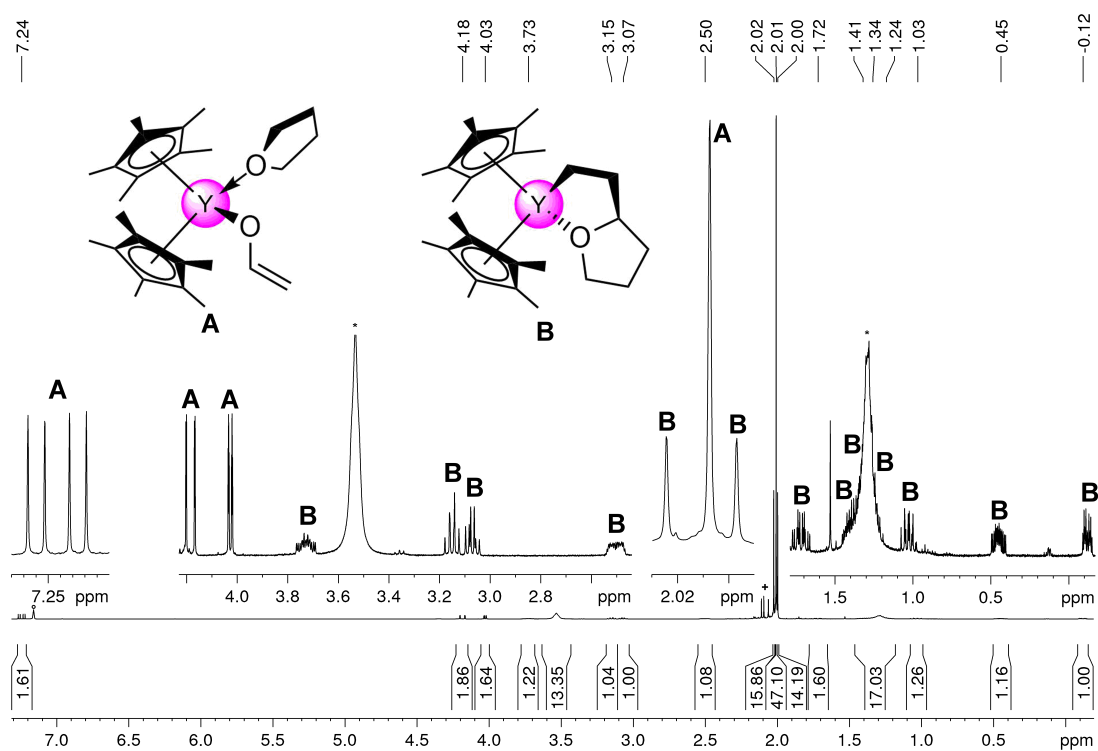


Figure S11. ^1H NMR spectrum (400 MHz) of crude product mixture of **2** and **3** in C_6D_6 at 26°C (* THF, + minor side products).

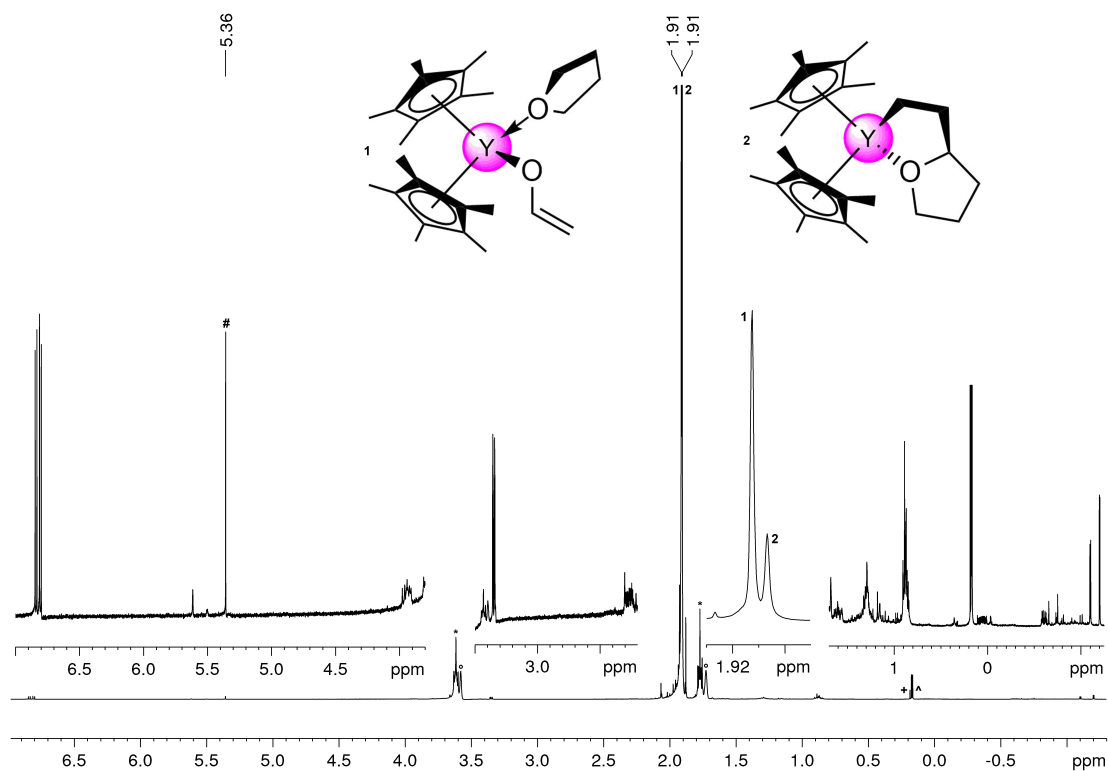


Figure S12. ^1H NMR spectrum (400 MHz) of crude product mixture of **2** and **3** in $\text{THF-}d_8$ at 26°C (* THF, # ethylene, + CH_4 , ^ CDH_3).

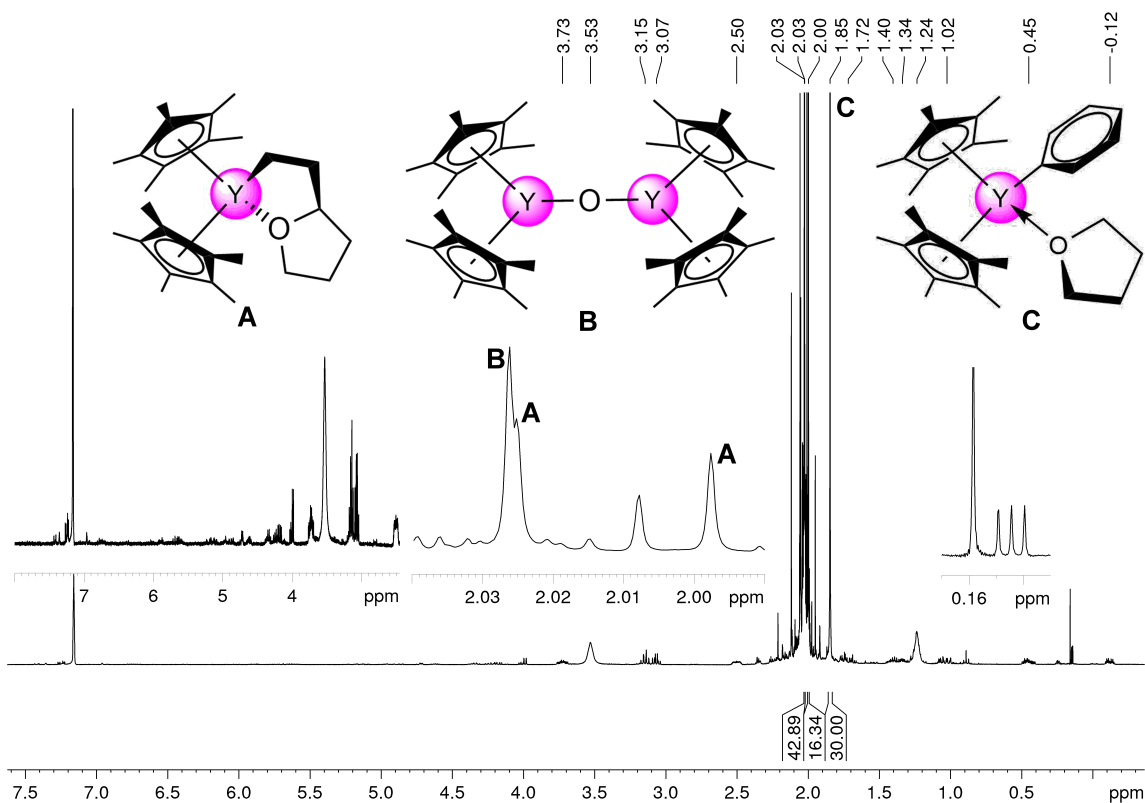


Figure S13. ^1H NMR spectrum (400 MHz) of **1** in C_6D_6 ($^\circ$) after heating to 90°C for 11 h. CH_4 and CDH_3 are formed in an approximate ratio of 1:1. Complex **2** is not detected

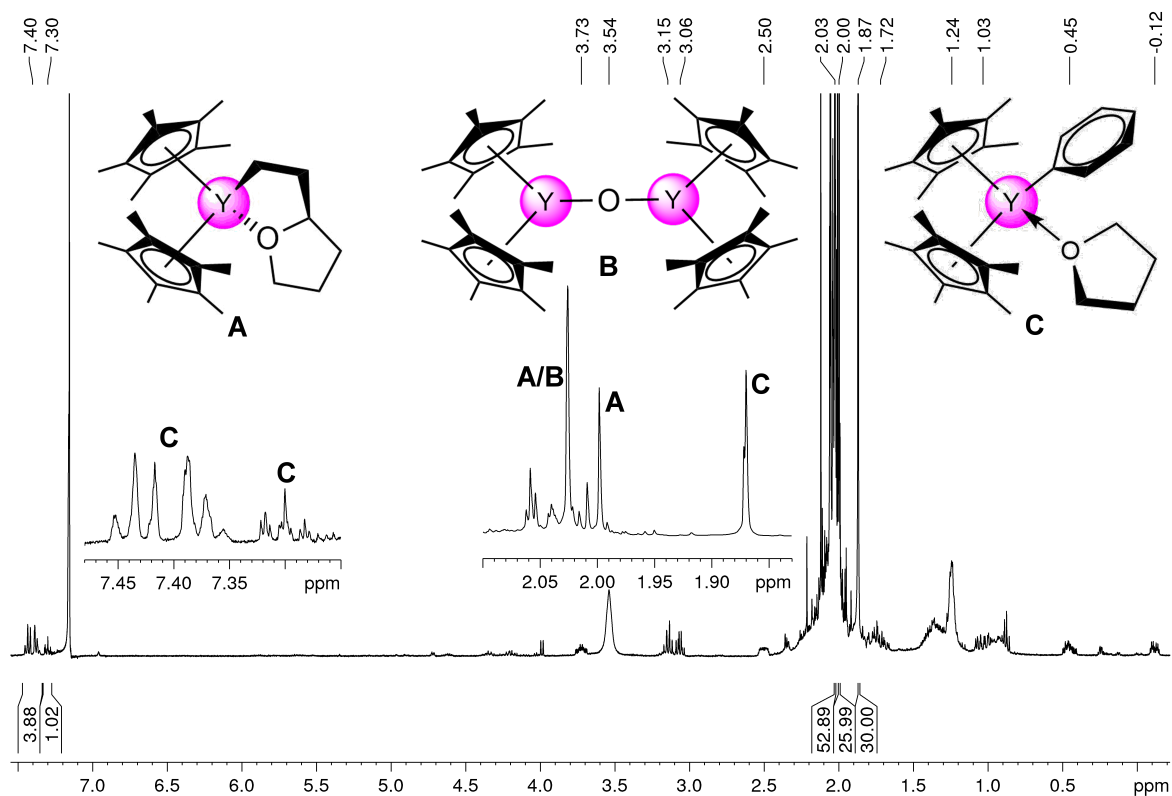


Figure S14. ^1H NMR spectrum (400 MHz) of **1** in C_6D_6 after heating to 90°C for 11 h, evaporation to dryness, extracting with C_6H_6 , evaporation to dryness and re-dissolving in C_6D_6 . Complex **2** is not detected.

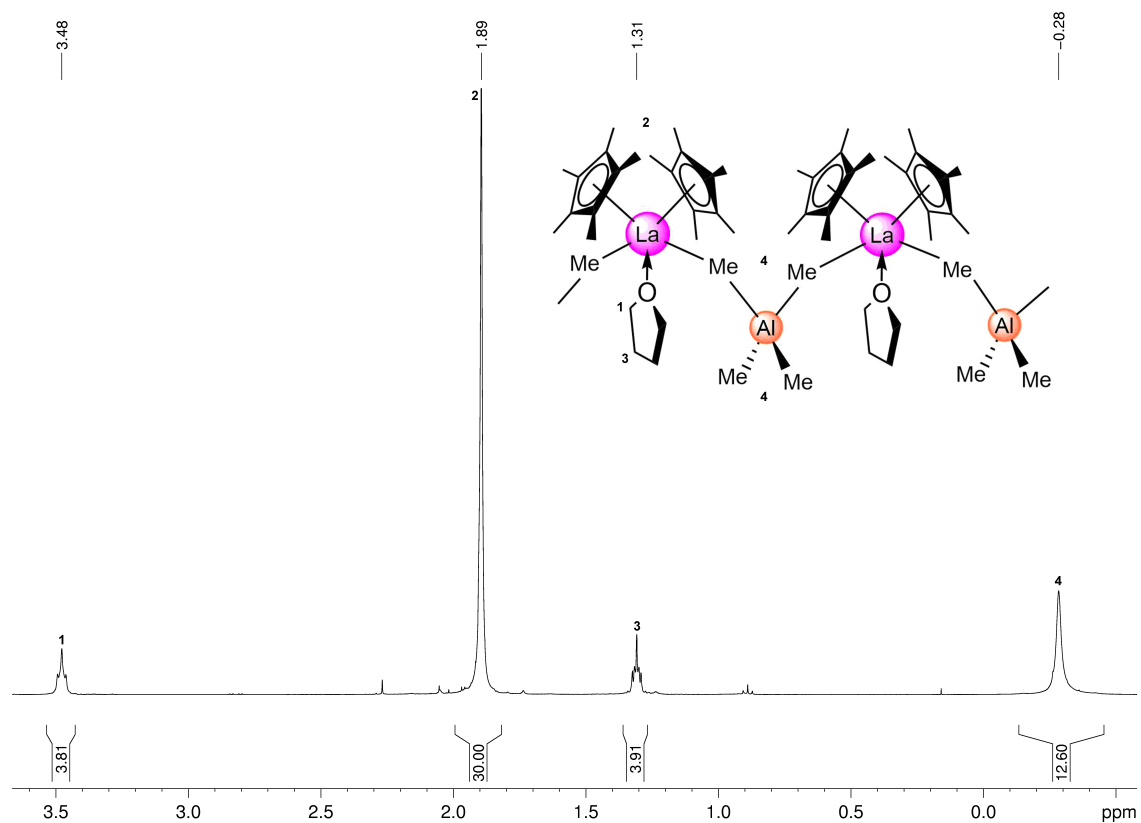


Figure S15. ^1H NMR spectrum (400 MHz) of **4** in C_6D_6 at 26°C .

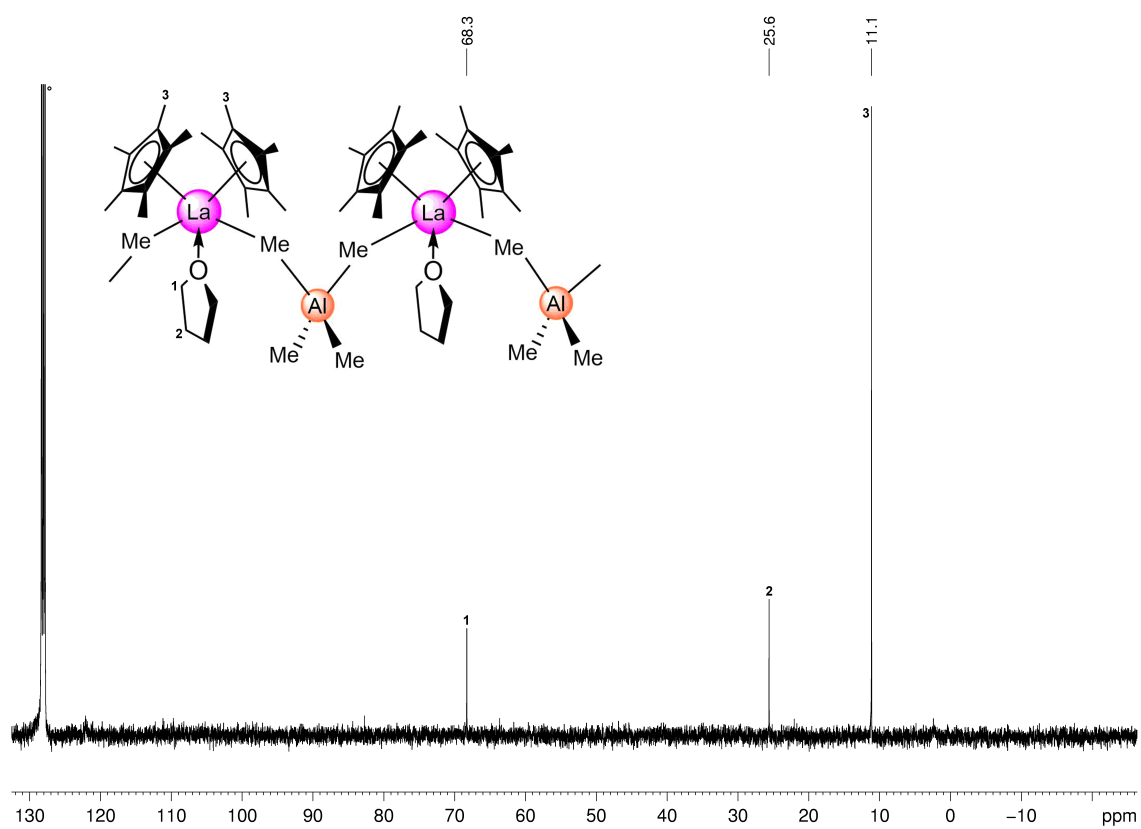


Figure S16. $^{13}\text{C}\{^1\text{H}\}$ NMR spectrum (101 MHz) of **4** in C_6D_6 at 26°C .

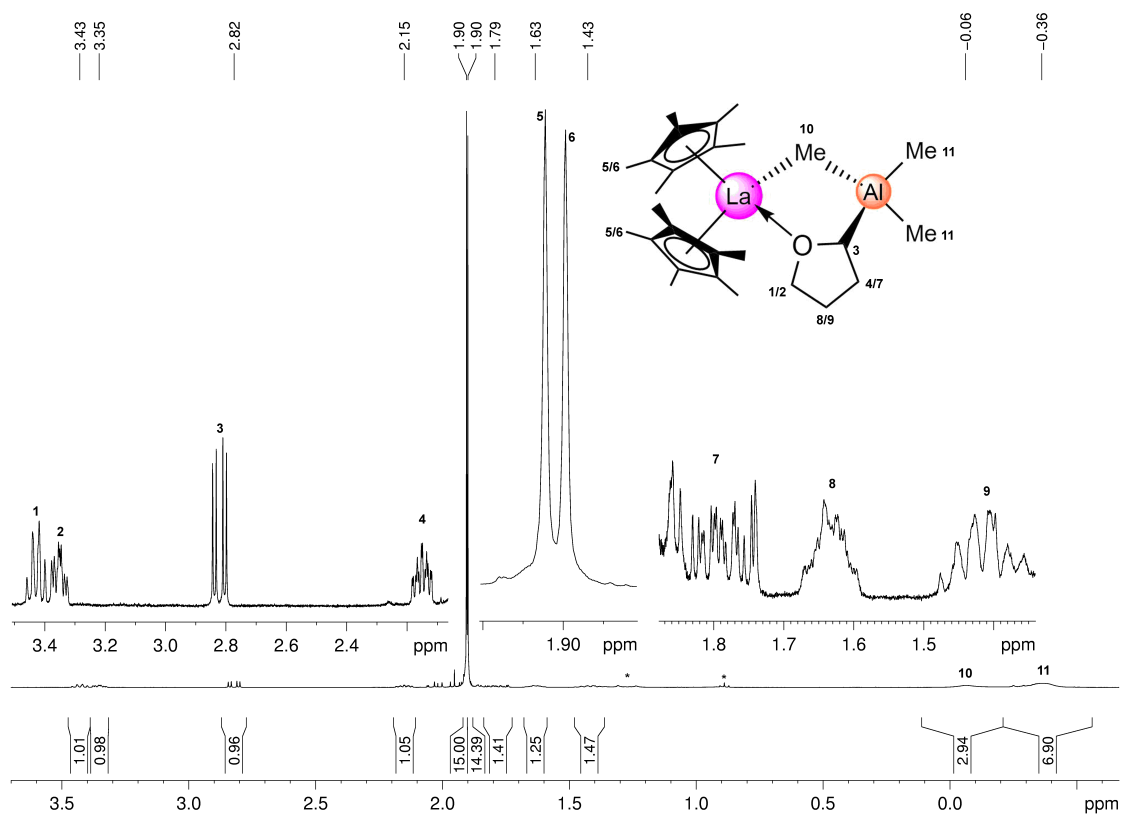


Figure S17. ^1H NMR spectrum (400 MHz) of **5** in C_6D_6 at 26°C .

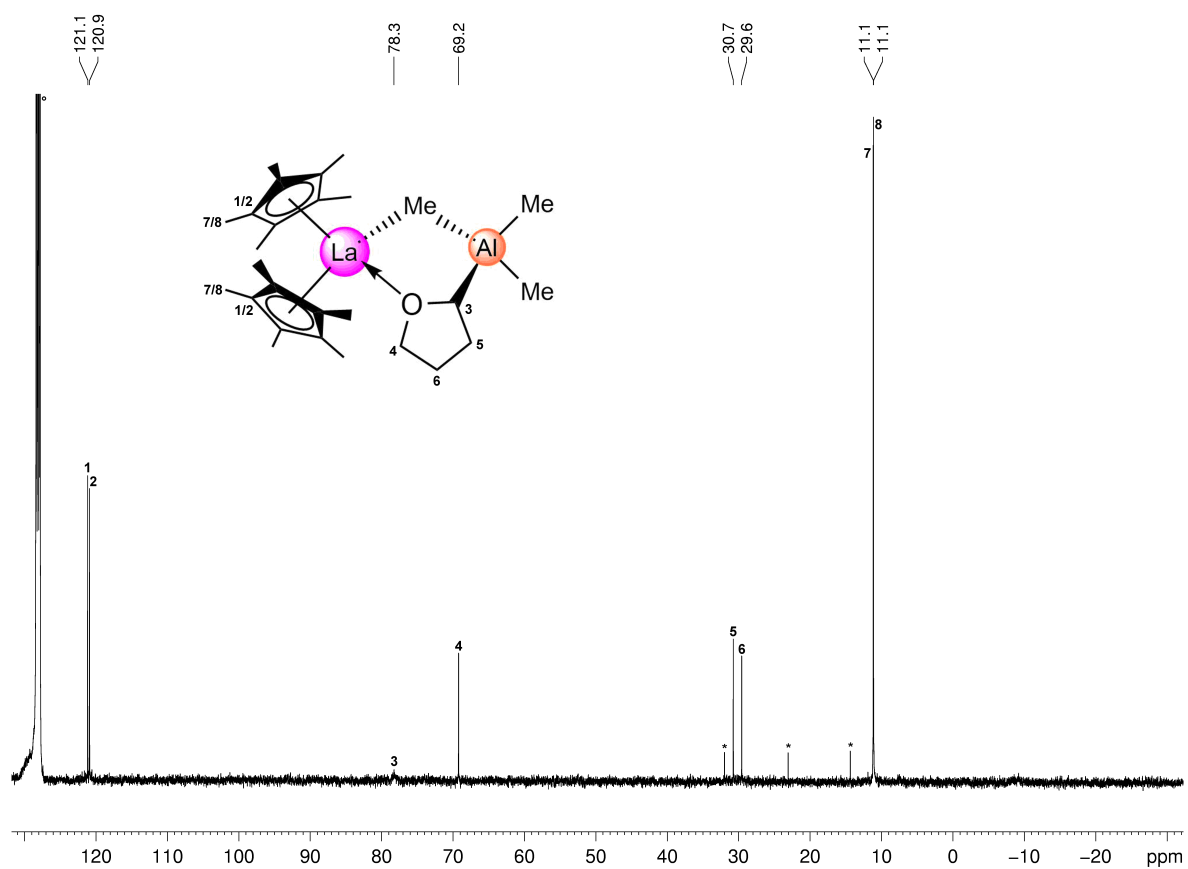


Figure S18. $^{13}\text{C}\{^1\text{H}\}$ NMR spectrum (101 MHz) of **5** in C_6D_6 ($^\circ$) at 26°C (* *n*-hexane).

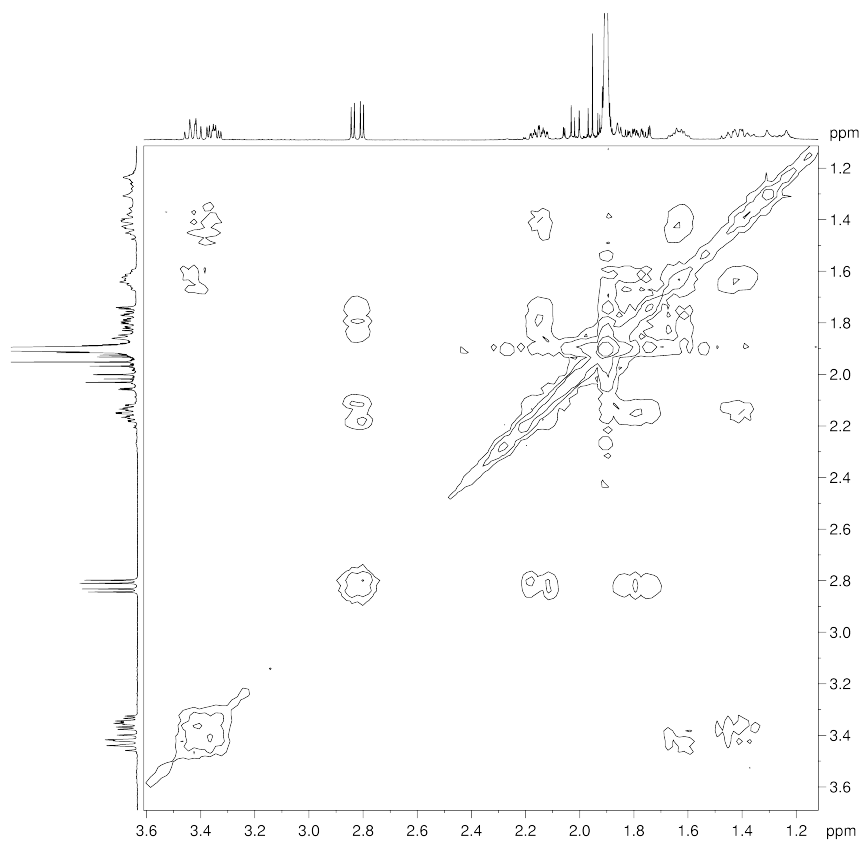


Figure S19. ^1H - ^1H COSY NMR spectrum (400 MHz) of **5** in C_6D_6 at 26 °C.

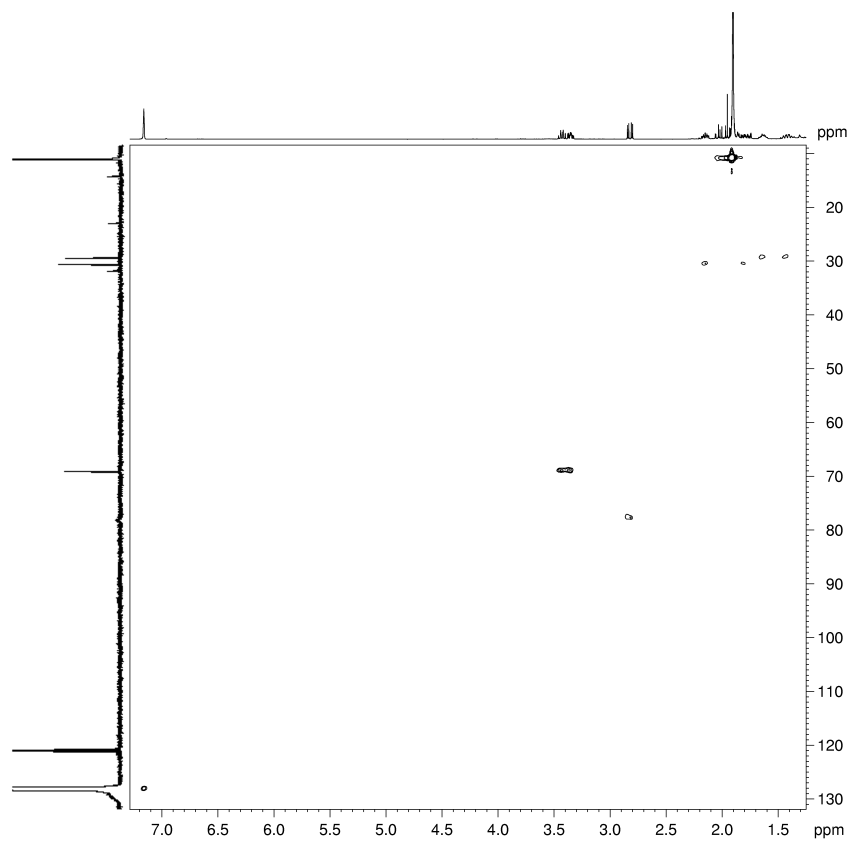


Figure S20. ^1H - ^{13}C HSQC NMR spectrum (400 MHz, 101 MHz) of **5** in C_6D_6 at 26 °C.

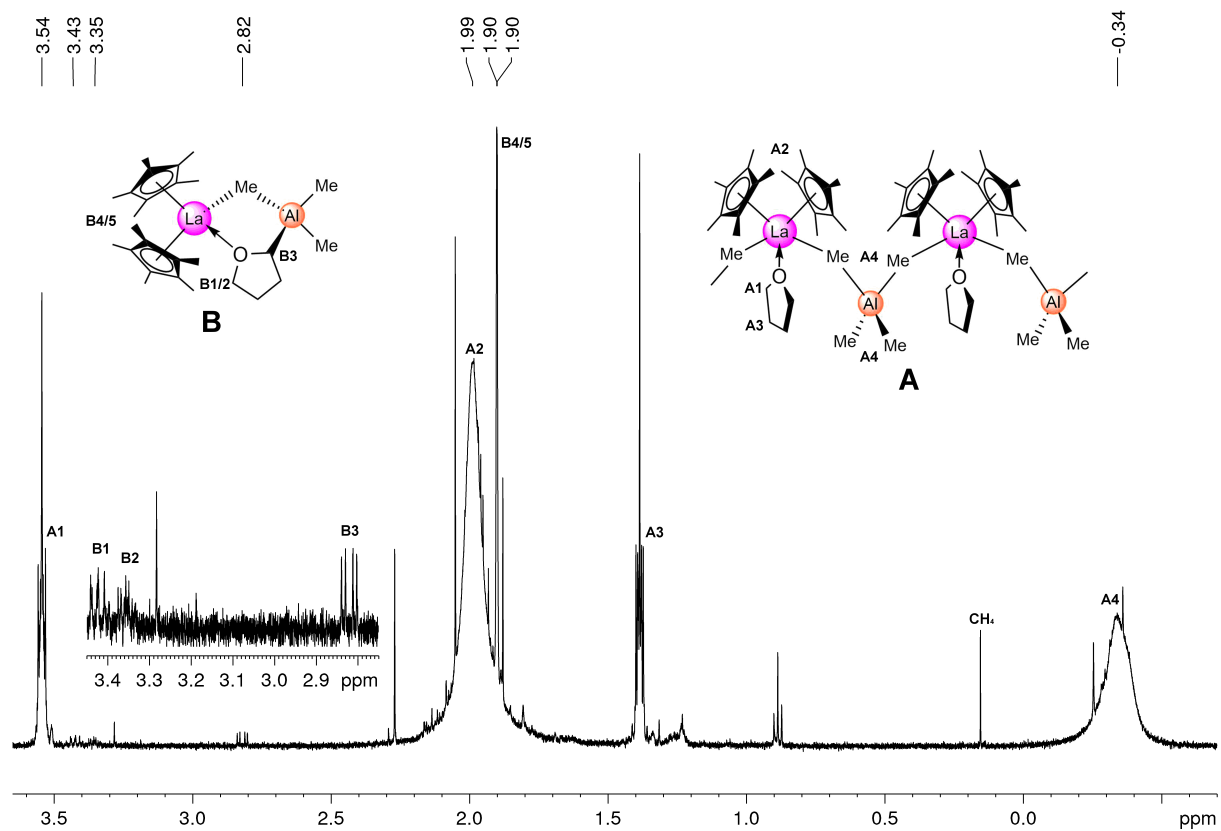


Figure S21. ^1H NMR spectrum (400 MHz) of 4 (A) in C_6D_6 at $26\text{ }^\circ\text{C}$, recorded after 1 h upon addition of some drops of $\text{THF-}d_8$, revealing the formation of methane and compound 5 (B).

References

1. H. M. Dietrich, K. W. Törnroos, E. Herdtweck and R. Anwander, *Organometallics*, 2009, **28**, 6739-6749.
2. COSMO, v. 1.61; Bruker AXS Inc.: Madison, WI, 2012.
3. APEX 3, v. 2017.3-0; Bruker AXS Inc., Madison, WI, 2017; APEX 2, v. 2012.10-0; Bruker AXS Inc., Madison, WI, 2012.
4. SAINT, v. 8.34A; Bruker AXS Inc., Madison, WI, 2013.
5. SHELXTL: G. M. Sheldrick, *Acta Crystallogr.*, 2015, **A71**, 3–8.
6. SHELXLE: C. B. Hübschle, G. M. Sheldrick and B. Dittrich, *J. Appl. Crystallogr.*, 2011, **44**, 1281-1284.
7. SADABS: L. Krause, R. Herbst-Irmer, G. M. Sheldrick and D. Stalke, *J. Appl. Crystallogr.* 2015, **48**, 3.
8. DSR: enhanced modelling and refinement of disordered structures with SHELXL: D. Kratzert, J. J. Holstein and I. Krossing, *J. Appl. Cryst.*, 2015, **48**, 933-938.
9. L. J. Farrugia, *J. Appl. Crystallogr.*, 1997, **30**, 565-566.
10. POV-Ray v. 3.6; Persistence of Vision Pty. Ltd.: Williamstown, Victoria, Australia, 2004. <http://www.povray.org/>.
11. K. H. Den Haan, J. L. De Boer, J. H. Teuben, W. J. J. Smeets and A. L. Spek, *J. Organomet. Chem.*, 1987, **327**, 31-38.
12. a) B.-J. Deelman, M. Booij, A. Meetsma, J. H. Teuben, H. Kooijman and A. L. Spek, *Organometallics*, 1995, **14**, 2306-2317; b) S. N. Ringelberg, A. Meetsma, S. I. Troyanov, B. Hessen and J. H. Teuben, *Organometallics*, 2002, **21**, 21759-1765.